

## Electronic Supplementary Information

# A surface-modified EDTA-reduced graphene oxide membrane for nanofiltration and anti-biofouling prepared by plasma post-treatment

*Byeongho Lee<sup>a,b</sup>, Dong Woo Suh<sup>a</sup>, Sung Pil Hong<sup>c</sup>, Jeyong Yoo<sup>a,d\*</sup>*

<sup>a</sup> School of Chemical and Biological Engineering, College of Engineering, Institute of Chemical Processes(ICP), Seoul National University(SNU), Gwanak-gu, Daehak-dong, , Seoul 151-742, Republic of Korea.

<sup>b</sup> Current address: Centre for advanced 2D materials, National University of Singapore, Singapore 117542

<sup>c</sup> WCU Program of Chemical Convergence for Energy & Environment, School of Chemical and Biological Engineering, College of Engineering, Institute of Chemical Process, Seoul National University, Gwanak-gu, Daehak-dong, Seoul 151-742, Republic of Korea.

<sup>d</sup> Korea Environment Institute, 370 Sicheong-daero, Sejong-si 30147, Republic of Korea

\*To whom correspondence should be addressed. E-mail: jeyong@snu.ac.kr (J. Y.)

Table S1. A summary of characteristics of ions and an organic molecule tested. Size in table means that cations<sup>1</sup>.

Molecule or ion	Concentration (mM)	Size (width or hydrated diameter) (nm)	Ionic diameter (nm)	Analyte charge
Methylene Blue	0.02	1.43×0.61×0.4	-	+
K <sub>3</sub> Fe(CN) <sub>6</sub>	1.5	0.95 [Fe(CN) <sub>6</sub> ] <sup>3-</sup>	-	-
MgCl <sub>2</sub>	10	0.86 (Mg <sup>2+</sup> )	0.86 (Mg <sup>2+</sup> )	+
NaCl	10	0.72 (Na <sup>+</sup> )	0.116 (Na <sup>+</sup> ) 0.099 (Cl <sup>-</sup> )	+
KCl	10	0.66 (K <sup>+</sup> )	0.152 (K <sup>+</sup> )	+

Table S2. A summary of interlayer spacing of EDTA-rGO, EDTA-GO, Normal-GO<sup>1</sup> and rGO<sup>2</sup> in dry and wetted state.

Membrane	Interlayer spacing (Å)	
	In dry	In wetted
EDTA-rGO	3.7	4.4
EDTA-GO	7.1	9
Normal GO	9	13
Normal rGO	3.4	-

Table S3. The basic information for NF 1 and NF 2.

Membrane	NF 1	NF 2
Material	Polyamide	
MWCO (Da)	200	200~300
Estimated pore size (nm)*	2.36	2.36-2.7
Thickness (um)	125	
Surface charge at pH 7 (mV)	-7.5	-11.5

\*Please note that the estimated pore size was calculated with MWCO in the table. This information was provided by the manufacturer of NF 1 and NF 2 (Toray chem. Inc.).

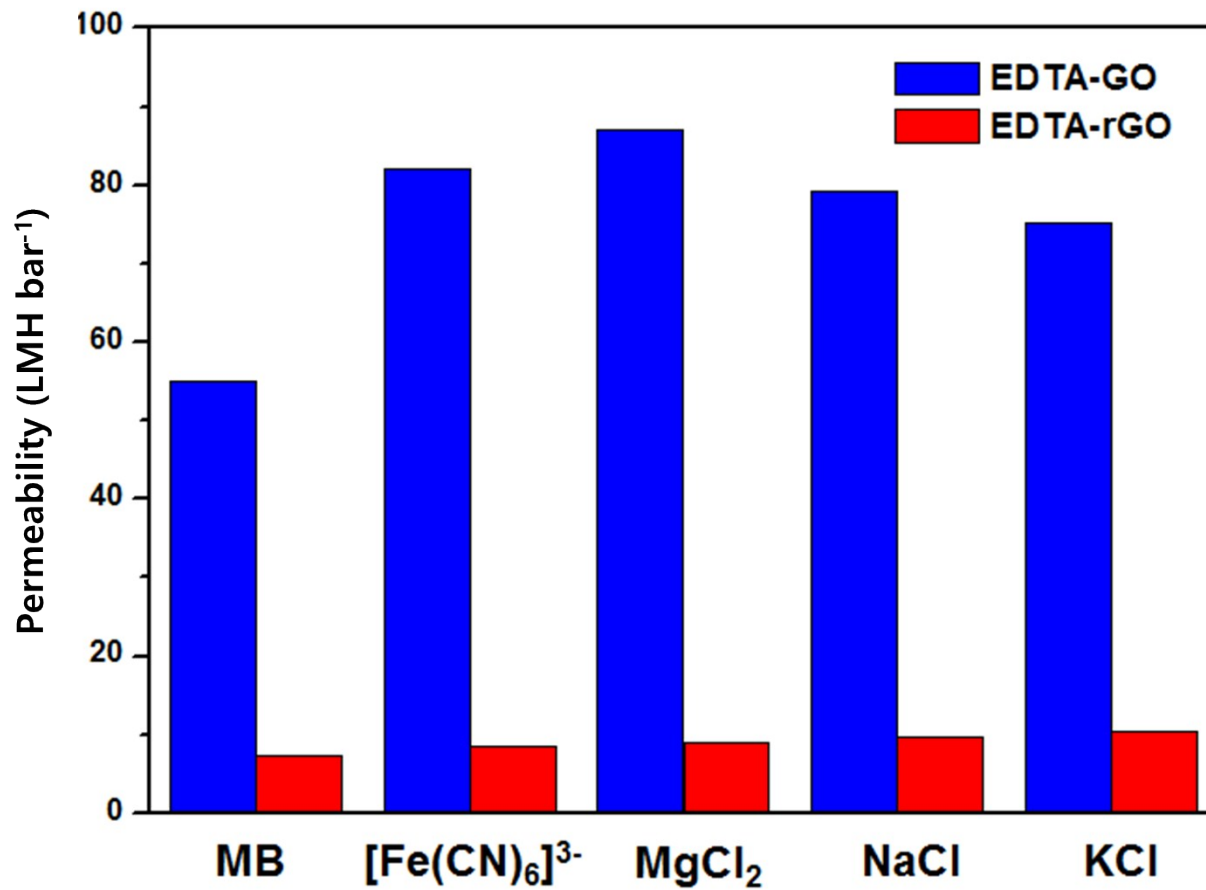


Figure S1 | Permeability of four ion solutions and an organic dye solution.

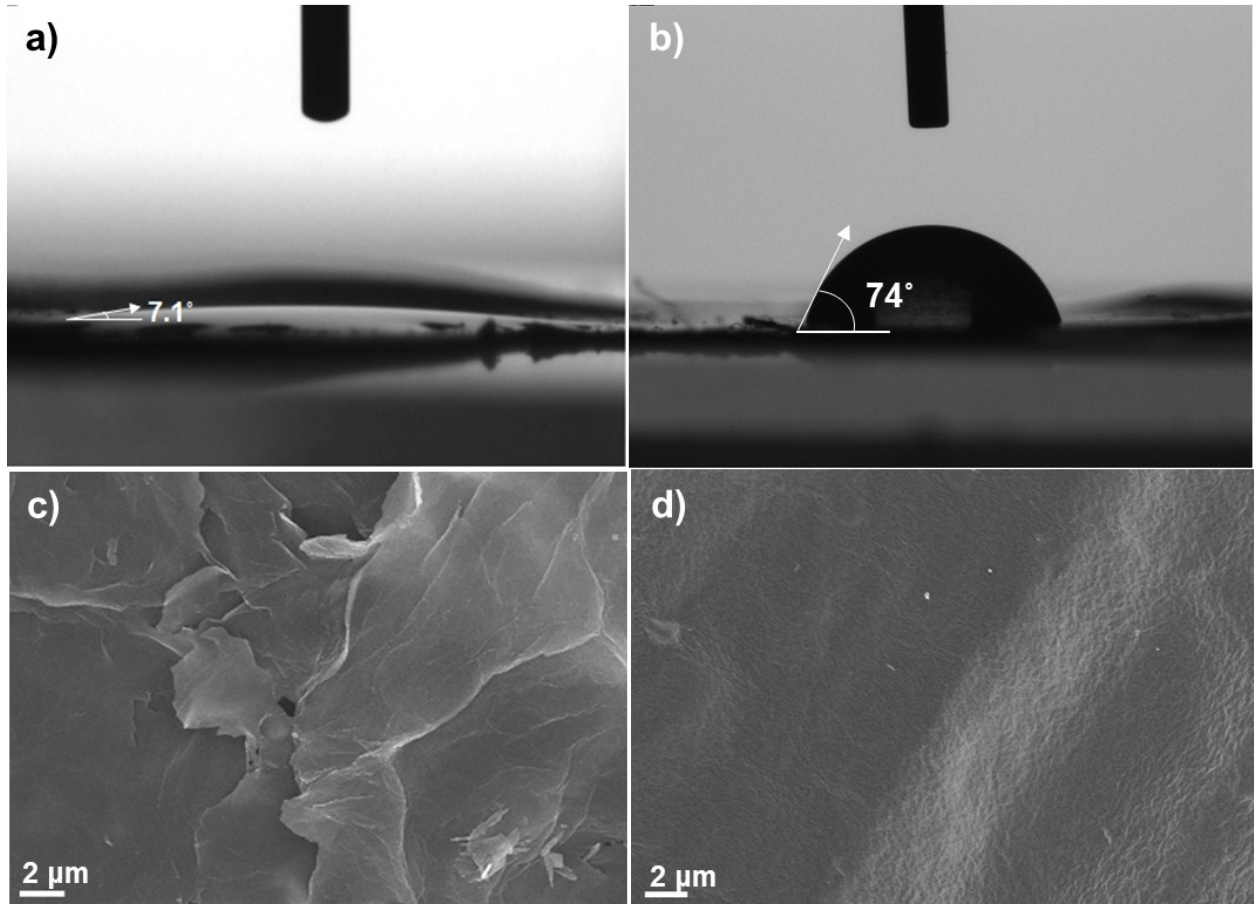


Figure S2 | Surface modification of P-EDTA-rGO and EDTA-rGO. Contact angles of water on (a) P-EDTA-rGO and (b) EDTA-rGO membrane and SEM images of the surface of (c) P-EDTA-rGO and (d) EDTA-rGO membrane on PTFE filter(support). Note that (a) and (c) are results on the P-EDTA-rGO treated with O<sub>2</sub>-plasma treatment for 180 sec.

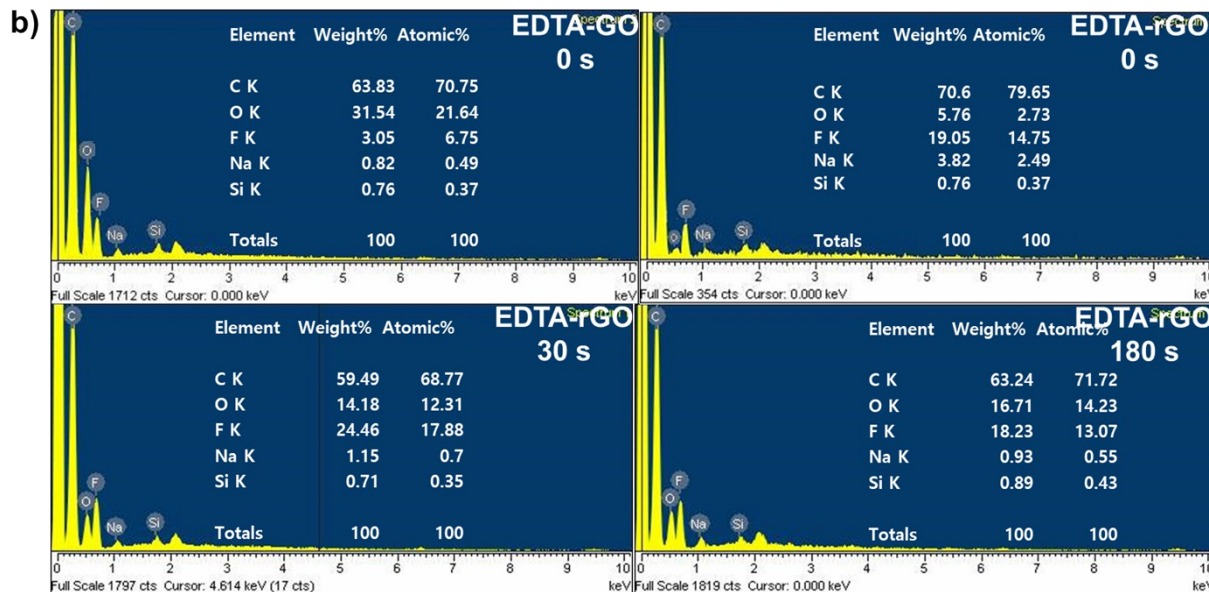
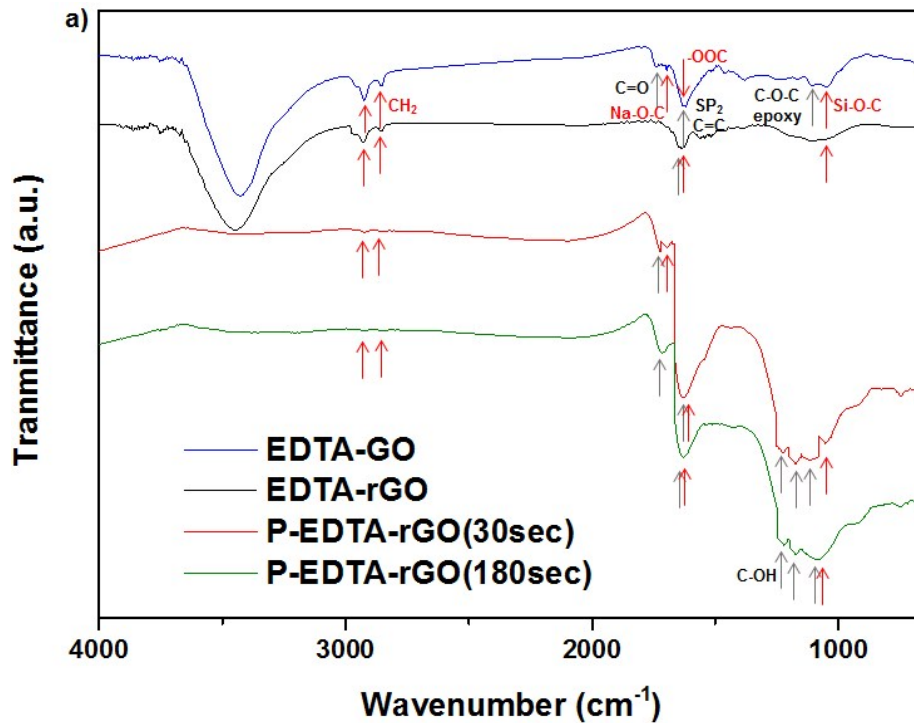


Figure S3 | Functional groups and elemental analysis after plasma treatment. a) FT-IR spectra of EDTA-GO, EDTA-rGO and P-EDTA-rGO (plasma treatment time: 30sec and 180sec). Gray arrows are for initial functional groups and  $\text{sp}^2$  bonding and the red ones are for EDTA peaks and bonding peaks between EDTA and graphene. b) EDS spectra of EDTA-GO, EDTA-rGO and P-

EDTA-rGO (plasma treatment time: 30sec and 180sec). Sodium and silicon peaks from EDTA are observed after the treatment. Fluorine peak comes from PTFE filter.

FTIR spectra demonstrates the addition of the oxygen functional groups after the plasma treatment (Fig. S3a). C=O ( $1733\text{ cm}^{-1}$ ), epoxy group ( $1174\text{ cm}^{-1}$ ), C-OH ( $1174\text{ cm}^{-1}$ ) and C-O ( $1060\text{ cm}^{-1}$ ), which are also found in graphene oxide<sup>3,4</sup>, were observed from the FT-IR spectra of P-EDTA-rGO which undergoes plasma treatment for 30 sec and 180 sec. EDTA molecules still exist on the P-EDTA-rGO sheets. Several peaks can be observed in the spectra of P-EDTA-rGO that undergoes plasma treatment for 30 sec and 180 sec, which indicates the presence of EDTA chain on the sheet surface. The two bands at approximately  $2900$  and  $2800\text{ cm}^{-1}$  in the spectra are associated with the stretching of the methylene groups of the EDTA molecules<sup>5</sup>. The band at  $1045\text{ cm}^{-1}$  in EDTA-GO spectrum and the band at  $1118\text{ cm}^{-1}$  in the spectra were assigned to the formation of Si-O-C<sup>5, 6</sup>. Sodium and Si backbone from EDTA molecule on the graphene is verified from EDS (energy dispersive spectroscopy, Fig. S3b) spectra after the plasma treatment. From the FTIR and EDS data, we conclude that surface of the P-EDTA-rGO membrane was functionalized with hydrophilic oxygen functional groups without loss of EDTA molecules. The surface of P-EDTA-rGO membrane became rough after the plasma treatment while the surface of EDTA-rGO was very smooth as observed by SEM (Fig S2c and d).



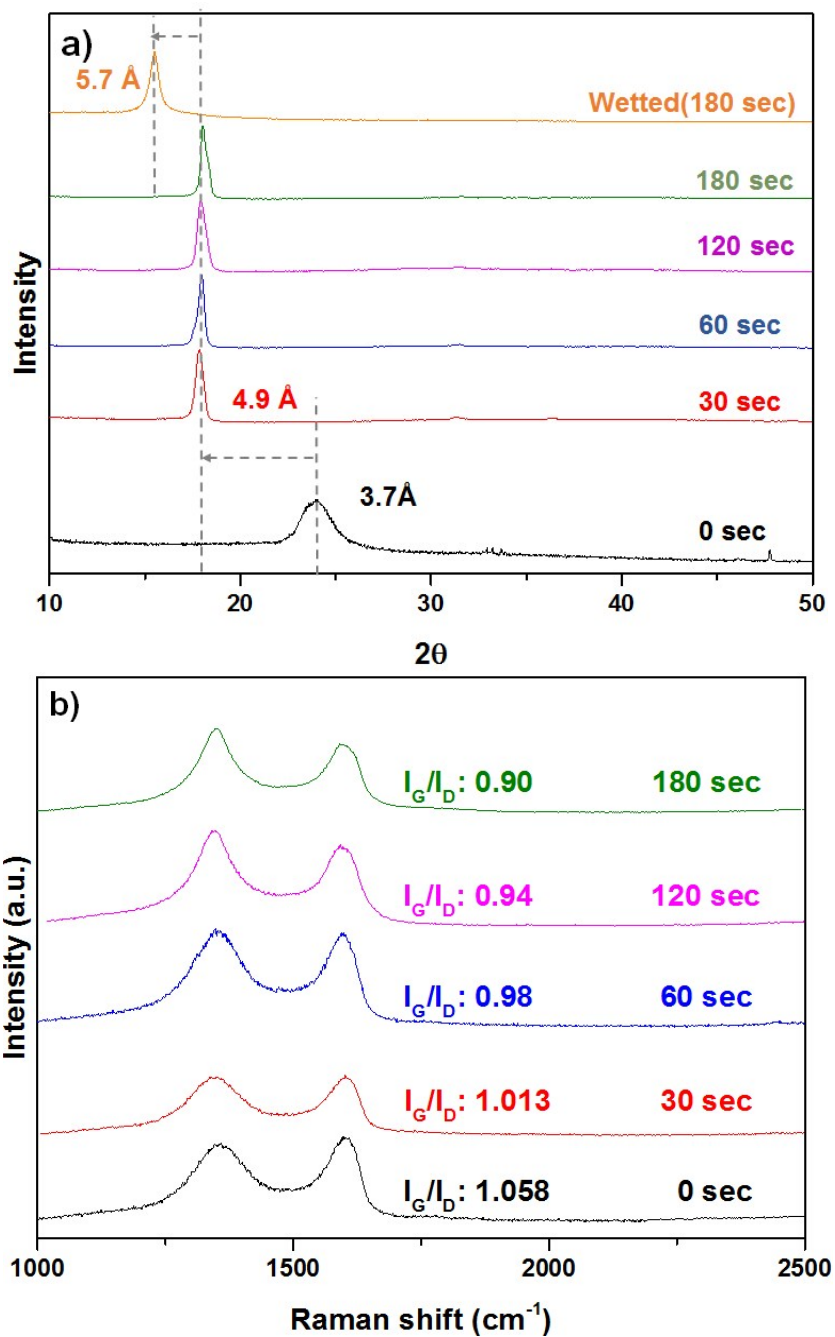


Figure S4 | Atomic structure analysis of EDTA-rGO membrane before and after the plasma treatment. a) X-ray diffraction results for P-EDTA-rGO according to plasma treatment time (30, 60, 120 and 180sec) and in wetted state. Note that XRD data in wetted state (orange color) are results on the P-EDTA-rGO membrane treated with  $\text{O}_2$ -plasma for 180 sec and black color curve

are from our previous paper<sup>4</sup> and b) Raman spectra of P-EDTA-rGO according to plasma treatment time (30, 60, 120 and 180sec).

The spacing increases from 3.7 Å to 4.9 Å after the treatment (Fig. S4a). It means that pore size of the membrane surface becomes larger. The widening of interlayer spacing could be due to the functional groups formed on the membrane surface after the treatment (Fig. S3a) and interlayer spacing of the P-EDTA-rGO membrane increases to 5.7 Å in wetted state (Fig. S4a). But, the interlayer spacing is still smaller than hydrated diameter of sodium and potassium ions.

The plasma treatment (or ion bombardment) can break up a graphene sheet to several pieces with smaller grain size. Therefore, the density of graphene edge on which the defects are concentrated increases. They would be shown as cracks on the membranes surface. We can clearly observe it from the SEM images (Fig. S5b). The ion bombardment can generate defects on the graphene sheets by breaking  $sp^2$  bonding between carbon atoms<sup>7</sup>. Water can pass through the cracks and defects that act as the membrane pores. Thus, increasing the crack and defects is desirable to increase the water permeability. Therefore, we conclude that the increase in hydrophilicity, pore density and interlayer spacing on the membrane surface led to improving the water permeability of P-EDTA-rGO.

Table S4. Summary of characteristics of EDTA-rGO and P-EDTA-rGO

Characteristics	EDTA-rGO	P-EDTA-rGO			
		Plasma treatment time(sec)			
		30	60	120	180
Permeability (LMH bar <sup>-1</sup> )	9.6	80	100	128	144
contact Angle (°)	74	33.7	27.3	9.3	7.1
I <sub>G</sub> /I <sub>D</sub>	1.058	1.013	0.98	0.94	9
Permeability(LMH·bar)	9.6	80	100	128	144
NaCl rejection (%)	83.7	-	-	-	81.4
Interlayer spacing (Å)	3.9	4.9			

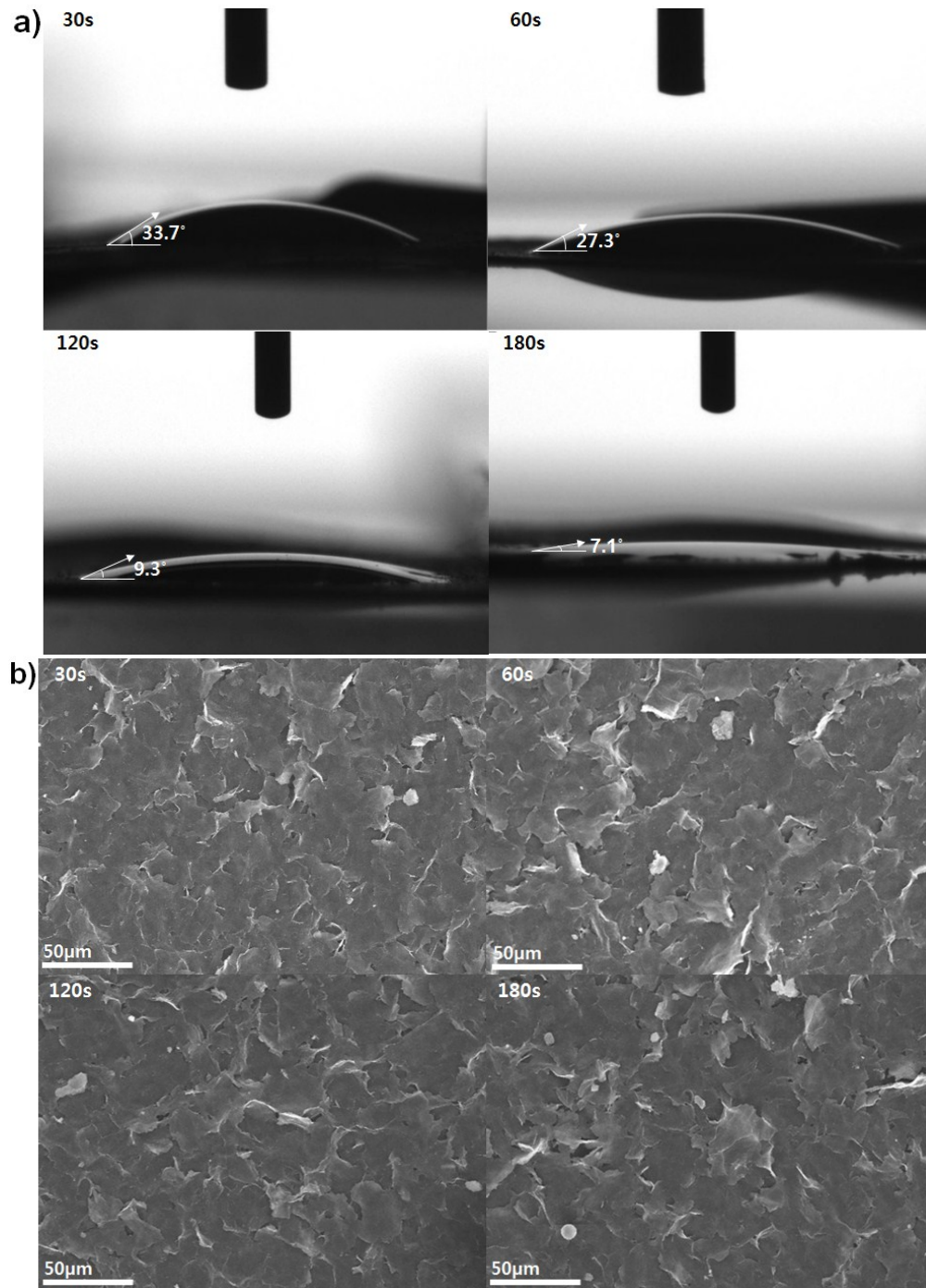


Figure S5 | Surface properties change of P-EDTA-rGO membrane according to plasma treatment time. a) A change in water contact angle on P-EDTA-rGO membrane according to plasma treatment time(30, 60, 120 and 180sec) and b) Surface SEM images of P-EDTA-rGO membrane on PTFE filter (support) according to plasma treatment time(30, 60, 120 and 180sec).

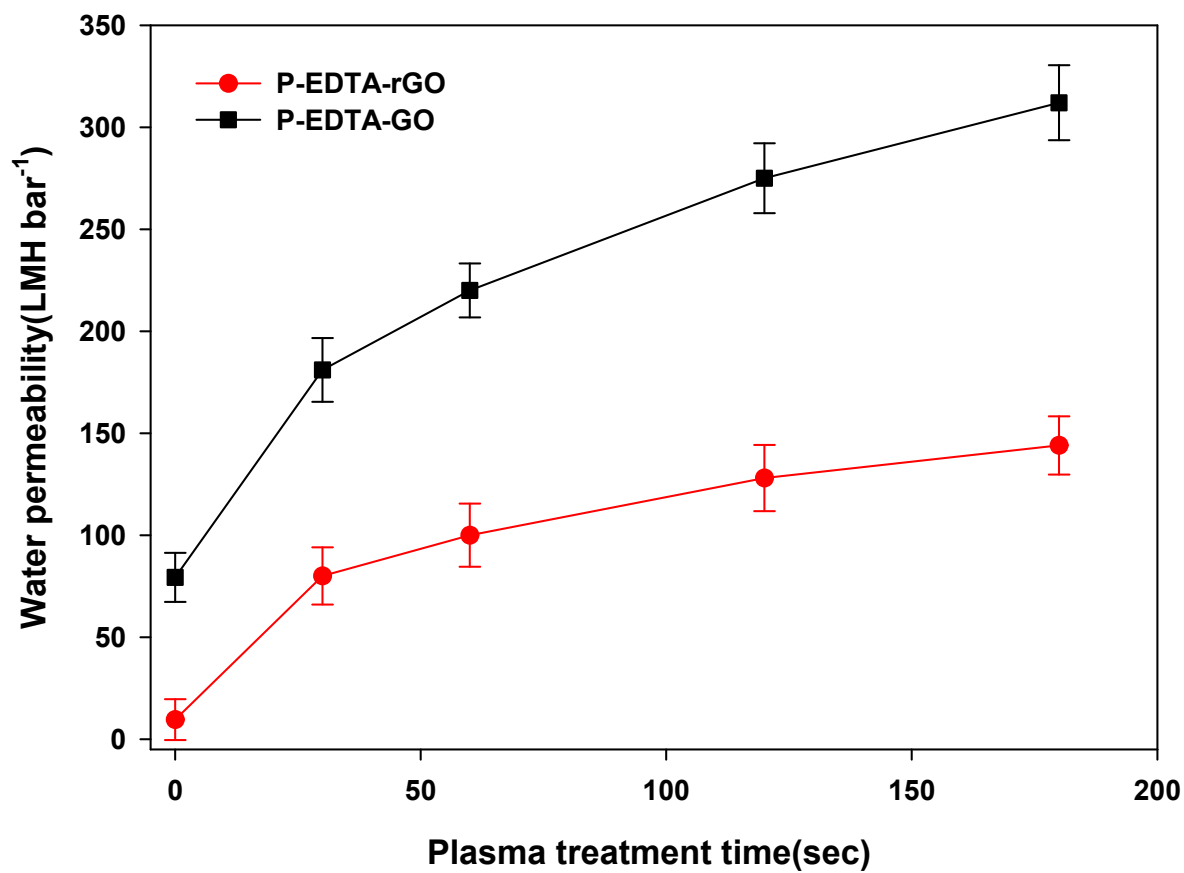


Figure S6 | Water permeability according to plasma treatment time (30, 60, 120 and 180sec). The permeability through P-EDTA-GO(black) and P-EDTA-rGO(red) was measured with NaCl aqueous solution.

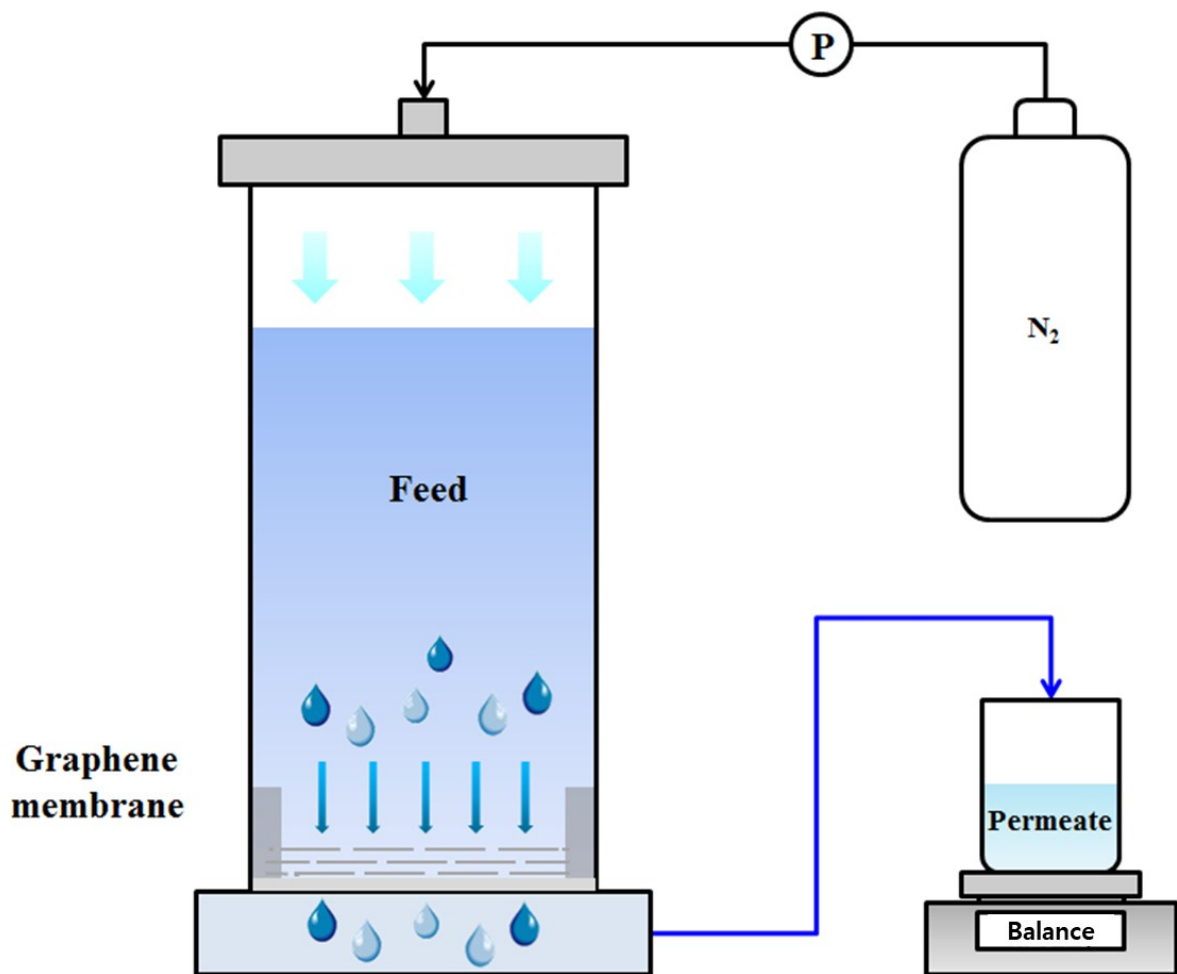


Figure S7 | A schematic of dead-end membrane filtration system. Water permeability and rejection tests were performed with N<sub>2</sub> gas at 15 bar. Permeate was collected and weighed. Water permeability was calculated from the information on permeate volume (mL), time and total membrane area.

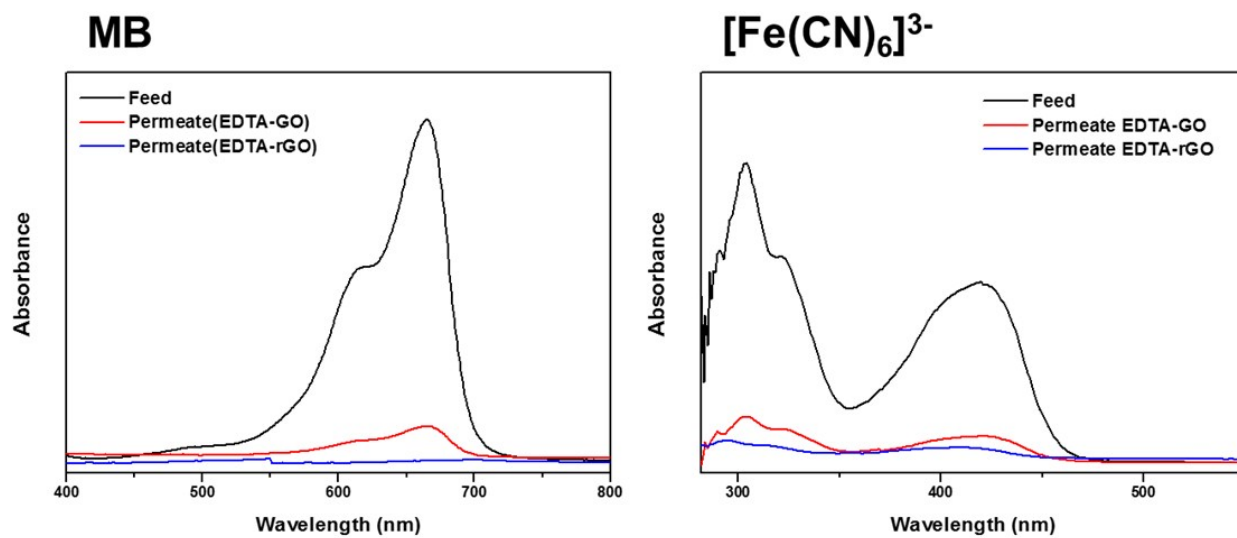


Figure S8 | UV-vis spectra of feed and permeate of MB and [Fe(CN)<sub>6</sub>]<sup>3-</sup> solution. Rejection rate for colored solution was estimated with ratio of maximum peak of feed and permeate before and after filtration (MB: 665 nm, [Fe(CN)<sub>6</sub>]<sup>3-</sup>: 305 nm)

## References

1. R. Joshi, P. Carbone, F. Wang, V. Kravets, Y. Su, I. Grigorieva, H. Wu, A. Geim and R. Nair, *Science*, 2014, **343**, 752-754.
2. Y. Su, V. Kravets, S. Wong, J. Waters, A. Geim and R. Nair, *Nature commun.*, 2014, **5**.
3. E.-Y. Choi, T. H. Han, J. Hong, J. E. Kim, S. H. Lee, H. W. Kim and S. O. Kim, *Journal of Materials Chemistry*, 2010, **20**, 1907-1912.
4. B. Lee, K. Li, H. S. Yoon, J. Yoon, Y. Mok, Y. Lee, H. H. Lee and Y. H. Kim, *Scientific Reports*, 2016, **6**.
5. S. Hou, S. Su, M. L. Kasner, P. Shah, K. Patel and C. J. Madarang, *Chem. Phys. Lett.*, 2010, **501**, 68-74.
6. T. Hemraj-Benny and S. S. Wong, *Chemistry of materials*, 2006, **18**, 4827-4839.
7. S. P. Surwade, S. N. Smirnov, I. V. Vlassiuk, R. R. Unocic, G. M. Veith, S. Dai and S. M. Mahurin, *Nature Nanotech.*, 2015, **10**, 459-464.